PHYSICAL REVIEW D

PARTICLES AND FIELDS

THIRD SERIES, VOLUME 34, NUMBER 3 1 AUGUST 1986

Study of hadron and inclusive muon production from e^+e^- annihilation at $39.79 \leq \sqrt{s} \leq 46.78$ GeV

B. Adeva,[f] S. Ansari,[d] U. Becker,[e] R. Becker-Szendy,[a] J. Berdugo,[f] A. Boehm,[a] J. G. Branson,[e] J. D. Burger,[e] M. Capell,[e] M. Cerrada,[f] C. C. Chang,[i] Y. H. Chang,[i] H. S. Chen,[i] M. Chen,[e,*] M. L. Chen,[i] M. Y. Chen,[i] Y. K. Chi,[i] E. Deffur,[a] K. Deiters,[j] M. Demarteau,[g] M. Dhina,[e] B. Z. Dong,[i] P. Duinker,[g] H. S. Fesefeldt,[a] D. Fong,[e] M. Fukushima,[e] L. Garrido,[f] R. D. Han,[i] D. Harting,[g] G. Herten,[e] M. C. Ho,[i] D. Hueser,[a] M. Hussain,[d] M. M. Ilyas,[e] D. Z. Jiang,[i] M. Klein,[j] W. Krenz,[a] P. Kuijer,[g] R. Leiste,[j] Q. Z. Li,[k] D. Linnhoefer,[a] D. Luckey,[e] E. J. Luit,[g] H. Ma,[c] C. Mana,[f] M. A. Marquina,[f] M. Martinez,[f] G. G. G. Massaro,[g] J. Mnich,[a] K. Nadeem,[d] H. Newman,[c] W. D. Nowak,[j] M. Nusbaumer,[h] M. Pohl,[k] F. P. Poschmann,[a] R. R. Rau,[b] S. Rodriguez,[f] M. Rohde,[d] J. A. Rubio,[f] H. Rykaczewski,[e] M. Sachwitz,[j] J. Salicio,[f] H. J. Schreiber,[j] U. Schroeder,[a] J. Schug,[a] H. Stone,[c] G. M. Swider,[g] H. W. Tang,[i] D. Teuchert,[a] Samuel C. C. Ting,[e] K. L. Tung,[i] H. Vogt,[j] M. Q. Wang,[i] M. White,[e] H. G. Wu,[i] S. X. Wu,[a] M. F. Wyne,[d] B. Wyslouch,[e] B. X. Yang,[i] X. Yu,[i] L. S. Zhang,[i] Z. H. Zhang,[i] B. Zhou,[e] and R. Y. Zhu[c]

[a]*III. Physikalisches Institut, Technische Hochschule, D-5100 Aachen, Federal Republic of Germany*

[b]*Brookhaven National Laboratory, Upton, New York 11973*

[c]*California Institute of Technology, Pasadena, California 91125*

[d]*Deutsches Elektronen Synchrotron, Notkestrasse 85, D-2000 Hamburg 52, Federal Republic of Germany*

[e]*Laboratory for Nuclear Science, Massachusetts Institute of Technology, Cambridge, Massachusetts 02139*

[f]*Junta de Energia Nuclear, Madrid, Spain*

[g]*Nationaal Instituut voor Kernfysica en Hoge-Energiefysica (NIKHEF), 1009-DB, Amsterdam, The Netherlands*

[h]*Universite de Geneve, 1211 Geneve 4, Switzerland*

[i]*Institute of High Energy Physics, Chinese Academy of Science, Peking, People's Republic of China*

[j]*Institut für Hochenergiephysik, Akademie der Wissenschaften der Deutschen Demokratischen Republik, 1615 Berlin-Zeuthen, Deutschen Demokratischen Republik*

[k]*Eidgenossisch-Technische Hochschule Zurich, CH 8093 Zurich, Switzerland*

(Received 27 January 1986)

We use the reaction $e^+e^- \rightarrow$hadrons, in the Mark J detector at the DESY electron-positron collider PETRA, to determine the hadronic cross section up to 46.78 GeV. The production of a top quark with a charge equal to $\frac{2}{3}$ is excluded up to 46.6 GeV with 95% C.L. The observed rise in the cross section at higher energies is consistent with the electroweak prediction for a Z^0 mass of 93 GeV. We describe some unusual muon inclusive events.

I. INTRODUCTION

PETRA, the electron-positron collider at DESY, has a maximum center-of-mass energy of 46.78 GeV. In this paper the Mark J collaboration reports results on hadron production in the highest-energy interval, $39.79 \leq \sqrt{s} \leq 46.78$ GeV (Ref. 1). The standard electroweak model[2] and quantum chromodynamics[3] (QCD) are, as of now completely successful in describing the electromagnetic, weak, and strong interactions. One prediction[4] which is not experimentally established as yet is the observation of a sixth (top) quark, with a positive electric charge equal in magnitude to $\frac{2}{3}$ that of the electron. Observation of the top quark would complete the postulated third family of quarks.[5]

We discuss data collection and analysis techniques in Sec. II. Section III outlines the determination of the total hadronic cross section and its use in the search for the top quark using both the cross section and event thrust distributions. Section IV addresses the electroweak effects. Section V focuses on some hadron events with unusual configurations and characteristics which contain at least one high-energy muon. Their origin remains unexplained.

For a general description of the Mark J detector and the analysis procedure see Ref. 1(a).

II. DATA COLLECTION AND ANALYSIS

The Mark J detector relies on calorimetry for multihadron event detection and measurement. The detector, for hadronic events, covers the azimuthal angle fully and the polar angle to $|\cos\theta| \leq 0.8$, with full energy containment. Particle detection and partial energy measurement is carried out to $|\cos\theta| \leq 0.98$.

Several triggers are employed to initiate the data collection procedures, but only two are significant for multihadron events. The hadron trigger relies on coincidences in several counter layers. The Bhabha trigger ($e^+e^- \rightarrow e^+e^-$) requires two groups of azimuthally opposed counters to record energy depositions. These triggers initiate the calculation of energy sums, which give information on the approximate total energy deposition in the calorimeter and the energy balance of these depositions. The total energy must exceed 20% of the center-of-mass energy.

Other triggers are used which select events containing muons or events with lower-energy depositions. Logically this set of triggers is 100% efficient, but hardware effects introduce losses which we find to be small enough to neglect.

Events recorded for off-line analysis are subject to a selection consisting of three stages. The first stage involves the use of a computer program that imposes loose criteria to remove triggered events which are obviously background. These involve simple minimum energy and energy balance criteria, and are more effective at eliminating background than the on-line triggers, since exact detector geometry and better pulse-height-to-energy-deposition conversion algorithms are employed. A second stage involves refined calibration constants and detailed reconstruction algorithms which reproduce the position and amount of the energy depositions accurately. In this case the position information from the drift tubes is used to determine the event vertex and gives a rough estimate of the charged multiplicity. This information, together with the ratio of the energy in the electromagnetic calorimeter to that in the hadron calorimeter, is used to separate events into four groups: (1) multihadron events; (2) Bhabha events; (3) background events; and (4) events which are ambiguous as to type. The multihadron and Bhabha samples are chosen using the shapes of the energy depositions within clusters of counters in conjunction with tracks reconstructed from the drift tubes. The ambiguous event sample is subjected to a third stage of analysis, involving an interactive graphics program which allows a physicist to inspect a visual reproduction of the detector with the pattern of energy depositions and charged-particle tracks superimposed. As these three processing stages are performed in parallel by two distinct analysis groups, detailed event-by-event comparisons of the selected data samples detect errors and allow estimates of uncertainties and biases.

Since the pulse-height-to-energy conversion factors change slowly with time we calibrate our detector in two steps. The pulse-height-to-energy factors are easily determined by the observation of the response of a counter to the passage of a single charged particle. Thus we include as part of our on-line data collection the recording of cosmic-ray muons which penetrate the detector. Since these muons are recorded with regular e^+e^- data, the time dependence of detector components is implicitly averaged over a period of about 2—4 weeks.

As a second step, the innermost three counter layers (for which a small error in the position of an energy deposition translates into a large angular error) are recalibrated using Bhabha events. These counters are 18 radiation lengths (r.l.) thick. The accurate position information obtained from the tracks reconstructed in the drift tubes can be compared to the position determined in the counters. The counter calibration constants correspondingly are varied to yield the best agreement. In this way we attain reproduction of event characteristics which are independent of slow time changes in counter characteristics.[6]

III. TOP-QUARK SEARCH

The reaction

$$e^+e^- \rightarrow \text{hadrons} \tag{1}$$

is used to search for the top quark and its cross section is expressed by the quantity R, defined as

$$R = \frac{\sigma(e^+e^- \rightarrow \text{hadrons})}{\sigma(\text{point})} , \tag{2}$$

where

$$\sigma(\text{point}) = 4\pi\alpha^2/3s = (86.85/s)\ \text{nb} ,$$

where s is in units of GeV^2. We select events from reaction (1) by requiring[7] that (a) the total visible energy E_{vis} is more than 50% of the c.m. energy, (b) the measured energy is balanced within 60% of E_{vis} in both longitudinal and transverse directions with respect to the beam line, and (c) the shape of the shower development in the layered structure of the detector is incompatible with a purely electromagnetic nature for the final state.

Using these selection criteria we determine the acceptance for reaction (1) to be 80—85 % over the PETRA energy range, with an uncertainty of about 1% at any energy. Thus it is essentially independent of energy and fragmentation models. Backgrounds from the τ decays and 2γ processes,

$$\begin{aligned} &e^+e^- \rightarrow \tau^+\tau^- \rightarrow \text{hadrons} + X , \\ &e^+e^- \rightarrow e^+e^- + \text{hadrons} , \end{aligned} \tag{3}$$

are calculated using Monte Carlo procedures to give a contribution of

$$\Delta R_{\tau\tau} = 0.18 \pm 0.01, \quad \Delta R_{\gamma\gamma} = 0.05 \pm 0.03 ,$$

and they are independent of c.m. energy. These contributions are subtracted. Background from Bhabha events is negligible. Our background estimates show no dependence on the center-of-mass energy.

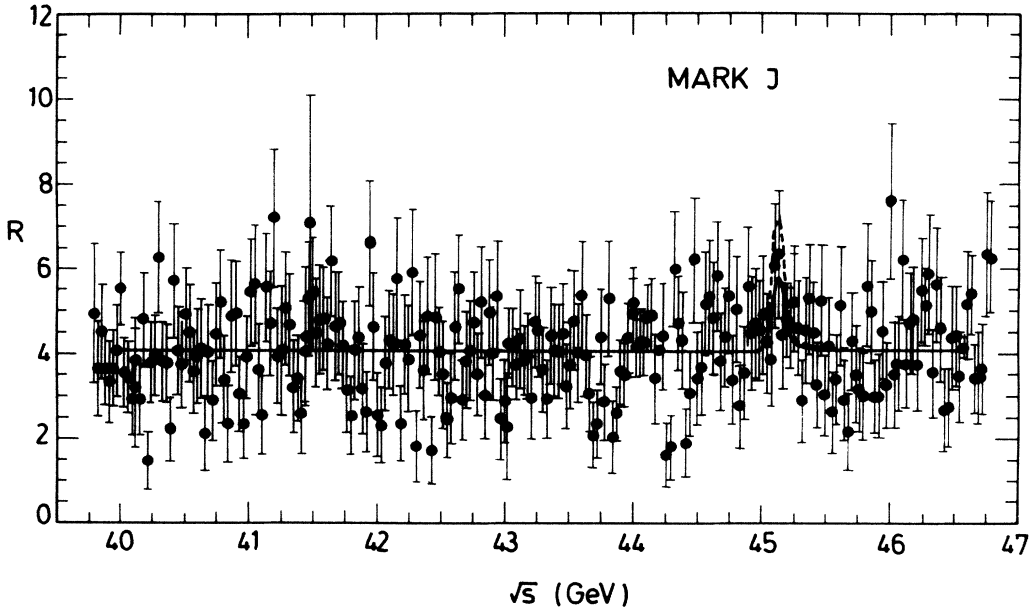

FIG. 1. R values are shown for the highest PETRA energies during an energy scan in 30-MeV steps.

A. Hadronic cross section R

The hadronic cross section is obtained by correcting the observed number of events for background contributions and for acceptance, and normalizing to the luminosity. In addition, corrections[8] for the effects of initial-state radiation are applied to present a cross section expressed as if no radiation effects were present. The net effect is to increase the number of events by 28% at 20 GeV and by 35% at 44 GeV. The luminosity is determined from Bhabha events. The electromagnetic calorimetry, covering $|\cos\theta| \leq 0.98$ records the processes $e^+e^- \to e^+e^-$, $e^+e^-\gamma$, $\gamma\gamma$, and $\gamma\gamma\gamma$. The rate and angular distributions for Bhabha events agree with the QED predictions.[1(a)] The luminosity values derived from our two separate analysis groups agree within 3%.

At specific energies, bound states (t-quarkonium) of the top quark and antiquark ($t\bar{t}$) should occur. At c.m. energies about 1—2 GeV above the ground state,[9] pairs of top mesons ($T^{\pm,0}$) would be produced and the hadronic cross section would increase.[10] For a top quark with a charge $+\frac{2}{3}$ and including QCD and electroweak corrections,[11] the total increase in R is expected to be $\Delta R \approx 1.5$ at energies sufficiently above threshold.

At PETRA, R has been determined by energy scans in which successive c.m. energy points were separated by 20-MeV steps below 38 GeV and by 30-MeV steps above 38 GeV (Ref. 12). Figure 1 presents all data from 39.79 to 46.78 GeV. Figure 2 is a plot of all data as a function of $\sqrt{s}$, summed into $\approx$1-GeV energy bins. The predicted value of R, is shown for 5 quarks (u,d,s,c,b) by the solid curve and for 6 quarks, including the charged $+\frac{2}{3}$ top quark, by the dashed curve. Our results show the slow increase in R at the highest energies, as predicted by the standard electroweak theory. The data and the 5-quark prediction are in excellent agreement to the highest PETRA energy. Measured R values for various energy bins are given in Table I.

We have also determined upper limits on the excess of the hadronic cross section, which we call ΔR. To determine this, we divide our data into subsamples ranging from a variable $(s_{\min})^{1/2}$ to $(s_{\max})^{1/2}=46.78$ GeV. For each subsample, we determine the number of hadronic events and the integrated luminosity ($\int L\,dt$). Using the predicted R (where we use $\alpha_s=0.12$ at $\sqrt{s}=44$ GeV and take $m_{Z^0}=93$ GeV, $\sin^2\theta_W=0.217$) for the 5-quark production, the number of expected events is calculated. From the actual number of measured events we obtain a 95%-C.L. upper limit, and then subtract the predicted number of events. This difference is an *upper* limit on the

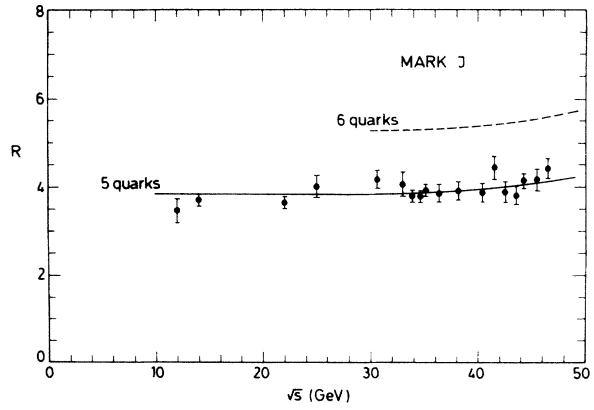

FIG. 2. R values averaged in $\approx$1-GeV bins for the entire PETRA energy region. The 5-quark prediction is shown by the solid curve; the 6-quark (including top) prediction by the dashed curve.

TABLE I. $\langle R \rangle$ values. The error quoted is the statistical error. Additionally there is a 3% point-to-point error and an overall (systematic) normalization error of 4%.

$\langle \sqrt{s} \rangle$ (GeV)	Number of events	$\int L\,dt$ (nb^{-1})	$\langle R \rangle$
12.00	224	98	3.47±0.25
14.03	2859	1572	3.71±0.07
21.99	2392	3234	3.55±0.08
25.00	402	610	4.03±0.21
30.61	915	2099	4.15±0.15
33.79	3739	10885	3.86±0.07
34.61	16464	51274	3.78±0.03
35.10	5616	17146	3.94±0.06
36.31	687	2270	3.88±0.16
37.40	147	544	3.59±0.32
38.38	512	1786	4.03±0.19
40.34	667	2729	3.87±0.16
41.50	515	1995	4.44±0.21
42.50	432	1904	3.89±0.20
43.46	582	2807	3.75±0.17
44.23	3410	15193	4.15±0.08
45.48	514	2385	4.17±0.19
46.47	776	3604	4.42±0.17

excess of measured events, which is then converted to an excess of the cross section, ΔR, as a function of the minimum c.m. energy, $(s_{\min})^{1/2}$. The result is shown in Fig. 3. These limits are valid for all models with hadronic final states regardless of the production scheme. [Note that we require reasonable energy balance; hence this statement does not include monojet events with very large unbalanced (missing) energy.] We are able to exclude an increase of the hadronic cross section predicted for full top-quark production ($\Delta R_{\text{top}} \approx 1.5$) up to an energy of $(s_{\min})^{1/2} = 46.6$ GeV at 95% C.L. Production of a pair of $\frac{1}{3}$ charge quarks is excluded for $(s_{\min})^{1/2} < 45.4$ GeV.

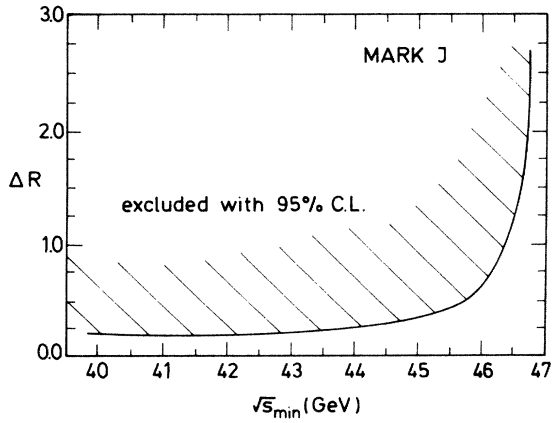

FIG. 3. A plot of ΔR, the (95% C.L.) excess of cross section from the data over the expected 5-quark cross section.

B. Resonant t-quarkonium states

The system of very narrow (compared to their masses) resonant states $(t\bar{t})$ formed by t quarks should be similar to the known $(c\bar{c})$ and $(b\bar{b})$ states.[13] They are predicted to be produced at a large cross section and have electronic decay widths $\Gamma_{ee} \approx 5$–10 keV (Ref. 14). They should decay into leptons or hadrons:

$$e^+e^- \rightarrow (t\bar{t}) \rightarrow \begin{cases} l^+l^- \\ \text{hadrons} \end{cases} . \tag{4}$$

For a t-quarkonium mass $(M_{t\bar{t}})$ in the PETRA energy range, the expected branching ratios are $\approx 32\%$ for leptons and 68% for hadrons assuming $\alpha_s \approx 0.12$ (Ref. 15) at highest PETRA energies.

We have searched for the t-quarkonium states in the latest energy scan between 39.79 and 46.78 GeV. These states should be observable as narrow resonances with experimental widths determined by the energy spread of PETRA, since the predicted t-quarkonium width is small compared with the 35-MeV energy spread. With these conditions the enhancement in R is expected to be a factor of 2–4 for a quark charge of $\frac{2}{3}$.

We determine the production cross section of a narrow resonance by fitting our data with the function[16]

$$R = R_0 + R_{\text{res}}(M_X, B_h \Gamma_{ee}) , \tag{5}$$

where R_0 is the continuum cross section, M_X the mass of the hypothetical resonance, B_h the branching ratio into hadronic final states, and Γ_{ee} the decay width into electrons. The function R_{res} describes the t-quarkonium resonance after correcting for machine energy resolution and radiative effects.

In Fig. 4 we show our measurements on an expanded energy scale from 44 to 46 GeV, and note that the most significant candidate for a resonance is at 45.12 GeV. Equation (5) is used to fit this energy region and we find

$$B_h \Gamma_{ee} \leq 3.00 \text{ keV} \quad \text{at 95\% C.L.} ,$$

which is to be compared with theoretically predicted values ranging from 3.5 to 7 keV (Ref. 14) for the ground state of t quarkonium. The solid curve in Fig. 4 indicates the best fit of Eq. (5), whereas the dashed curve represents the expected shape using the 95%-C.L. upper limit on $B_h \Gamma_{ee}$.

However, when determining the hadronic cross section R, we use the acceptance and the initial-state radiative corrections for the continuum cross section in measuring the production cross section of 5 quarks. In the presence of a resonance these corrections must be modified. When applying the relevant corrections to the resonant part of the measured cross section, this part of R (R_{res}) is reduced by a factor of about 1.33. This directly affects our fitted value of $B_h \Gamma_{ee}$ which must be increased by the same factor. (This factor is included in the 3-keV limit.)

We note that the expected electronic width of a $-\frac{1}{3}$ charge quark is approximately one-fourth that of the $+\frac{2}{3}$ charge quark. Thus, the height of a $-\frac{1}{3}$ quark charge resonance is too small to be resolved with the luminosity collected at each point.

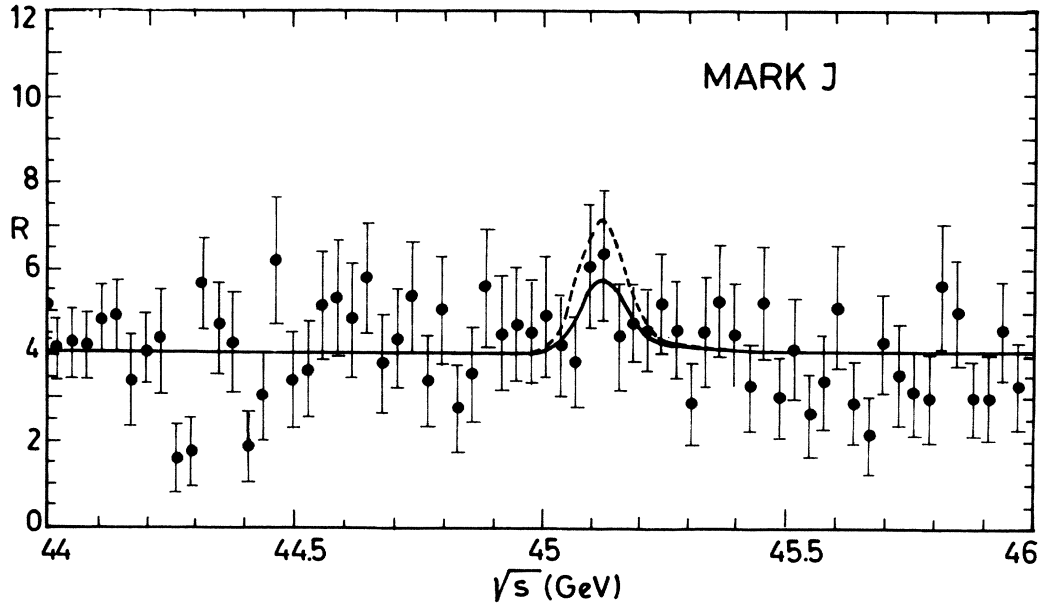

FIG. 4. The energy scan from 44 to 46 GeV contains the most significant candidate for the ground-state t-quarkonium resonance at 45.12 GeV. The continuous curve is the fit to $R = R_0 + R_{\rm res}$, including the PETRA c.m. energy spread and radiative effects. The dashed curve indicates the expected cross section using the 95%-C.L. upper limit on $B_h \Gamma_{ee}$.

C. Event topology

A third method for observing top-quark production is to analyze the event topology. We investigate our data using the thrust distribution, which for the Mark J data analysis, is defined as

$$T = \max \left[\sum | E_i e_1 | \Big/ \sum | E_i | \right], \tag{6}$$

where E_i is the energy flow vector of a particle or a group of particles hitting the ith element of the calorimeter. The unit vector e_1 is varied in direction until the right-hand side of (6) is maximized. If a virtual photon materialized into a quark-antiquark pair each with a mass close to the beam energy, the quarks would be produced nearly at rest and, hence, fragmentation into hadrons would be isotropic. In this case, T approaches 0.5 as a limit. For a quark-antiquark pair, produced far above threshold, the Lorentz transformation of their hadronic fragmentation products to the laboratory frame results in a hadron jet collimated around each of the initial-quark directions. As the beam energy increases the jets become narrower and T approaches 1. Thus, if a new quark threshold is crossed, the thrust distribution should show an enhancement at low-thrust values. Naturally, the argument applies to the threshold for any pair of heavy particles which decay primarily into multihadrons.

In our search for new hadronic states at the highest PETRA energies, we combine R and T and determine the thrust distributions normalized to the measured values of R and not to unity. This method gives the most sensitivity to our search. We also divide the data so as to maximize changes in R (ΔR). Thus we use two energy intervals: (1) 39.79—46.3 GeV; (2) 46.3—46.78 GeV. Figures 5 and 6 give dR/dT data and Monte Carlo distributions for 5 and 6 quarks as a function of thrust for the two energy regions.

Figure 5 shows the excellent agreement, for all thrust values, between our data and the 5-quark Monte Carlo calculation for the lower-energy region. Our data for $\sqrt{s} \geq 46.3$ GeV, Fig. 6, shows an enhancement of low-thrust events. In order to provide a measure of this enhancement, we use the cross section normalized to the QED point cross section and integrate over the low-thrust region, $0.5 < T < 0.75$. We designate the derived parameter as $R_{0.75}$. For $\sqrt{s} > 46.3$ GeV, $R_{0.75} = 0.43 \pm 0.06$

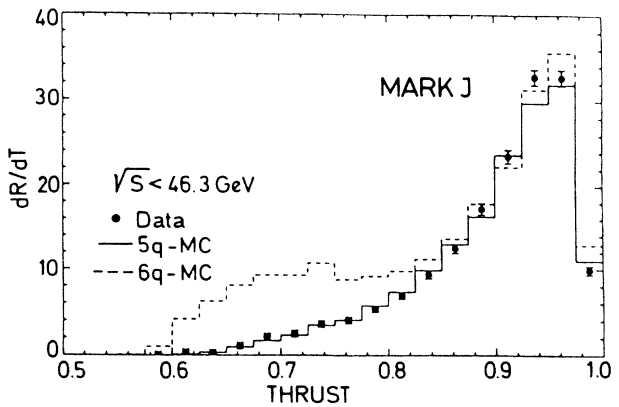

FIG. 5. dR/dT is given as a function of T (thrust) for $39.79 \leq \sqrt{s} < 46.3$ GeV.

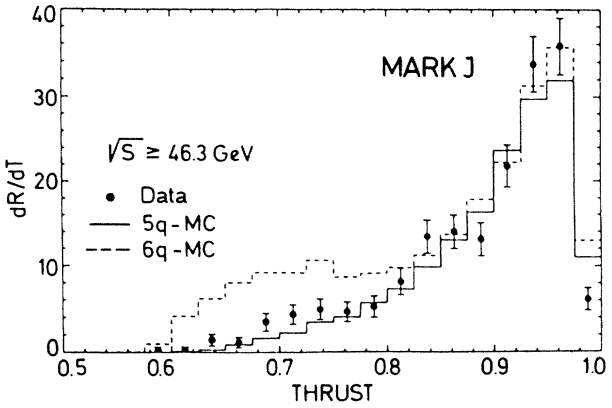

FIG. 6. dR/dT is given as a function of T (thrust) for $\sqrt{s} \geq 46.3$ GeV.

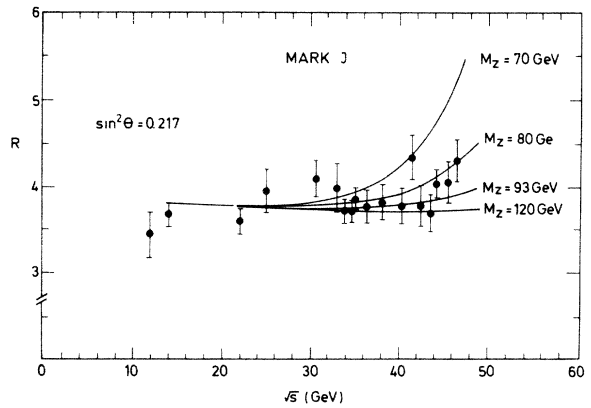

FIG. 7. R as a function of $\sqrt{s}$, with curves superimposed for different masses of the Z^0; $\sin^2\theta_W = 0.217$ is taken as given.

which is to be compared with the expected value for 5 quarks, $R_{0.75} = 0.21$, and for 6 quarks, $R_{0.75} = 1.21$, well above threshold. This measure of the observed deviation is in better agreement with the 5-quark expectation. (We discuss unusual events in this energy interval and thrust region in Sec. V.)

IV. ELECTROWEAK EFFECTS IN HADRON EVENTS

In Fig. 2 it can be seen that the hadronic cross section is rising slowly with increasing c.m. energy. R can be calculated, in the quark-parton model, without QCD and mass-effect corrections, but taking into account the exchange of γ, Z^0, and their interference, as[11]

$$R_q = 3 \sum_q [e_q^2 - 2e_q \chi s g_V^e g_V^q + \chi^2 s^2 | (g_V^e)^2 + (g_A^e)^2 | | (g_V^q)^2 + (g_A^q)^2 |] , \quad (7)$$

where

$$\chi = \frac{1}{4 \sin^2\theta_W \cos^2\theta_W} \frac{1}{s - m_{Z^0}^2} .$$

g_V^e and g_A^e are the electron-vector and axial-vector coupling constants, $g_V^q = \pm\frac{1}{2} - 2e_q \sin^2\theta_W$, and $g_A^q = \pm\frac{1}{2}$, where the plus sign is for $e_q = +\frac{2}{3}$, the minus for $e_q = -\frac{1}{3}$.

In Eq. (11) the first term describes the γ exchange, the second is the γ, Z^0 interference, and the third is the Z^0 exchange. The effect of QCD on R is generally small, and almost independent of energy. Thus, we choose to fix α_s at the value we determine from event shapes,[17] and concentrate on the electroweak effects.

From $\sqrt{s} = 35$ GeV to $\sqrt{s} = 44$ GeV we expect R to increase from 3.95 to 4.09. We observe $R = 3.94 \pm 0.06$ at 35 GeV and $R = 4.15 \pm 0.08$ at 44 GeV. Figure 7 shows the measured data points, grouped in 1-GeV bins, compared to curves from Eq. (11) for different Z^0 masses.

Using the R measurements displayed in Fig. 7 we perform a fit of Eq. (11), including QCD corrections, and obtain limits on the mass of the Z^0 taking the world average of $\sin^2\theta_W = 0.217 \pm 0.014$. We determine[18]

$$m_{Z^0} = 82^{+5}_{-3} \text{ GeV} ,$$

or with 95% C.L.,

$$76 \leq M_{Z^0} \leq 94 \text{ GeV} .$$

Figure 8 exhibits contours in the $\sin^2\theta_W$-m_{Z^0} plane.

Assuming the validity of the standard electroweak theory with $m_{Z^0} = 93$ GeV and $\sin^2\theta_W = 0.217$, we can extract limits on the pointlike nature of quarks from our data. We use the following form-factor parametrization of a deviation from QED:

$$F_\pm(s) = 1 \mp \frac{s}{s - \Lambda_\pm^2} . \quad (8)$$

We obtain $\Lambda_+ > 150$ GeV, $\Lambda_- > 350$ GeV at 95% C.L.

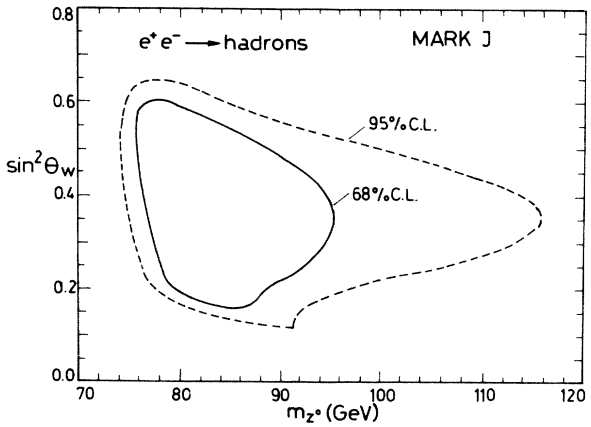

FIG. 8. χ^2 contours in the $\sin^2\theta_W$-Z^0 plane.

V. LOW-THRUST MUON-HADRON EVENTS ABOVE 46.3 GeV (REFS. 19 AND 20)

The reaction

$$e^+e^- \rightarrow \mu + \text{hadrons} \quad (9)$$

is not only an excellent signature for top-quark production, it is also a signature which could announce the production of other new particles, for example, new leptons. We have used the rate of inclusive muon events at low thrust, $T < 0.8$, as an indicator of new particle production. See Ref. 1(a).

Muons are measured in the Mark J detector[1(a),19] by using large-area drift chambers installed behind an iron absorber of about 90 c.m. thickness. As a consequence of this hadron filter only muons with a momentum exceeding 1.5 GeV/c can reach the outer chambers. Unfortunately not all muons detected in the outer drift chambers originate from heavy-quark decays, but also from π and K decays. Further background comes from hadronic events where typically a pion punches through the iron absorber without creating a hadron shower, and fakes a muon.

The cross section for inclusive muon events, with $T < 0.8$ is plotted in Fig. 9 as a function of the c.m. energy from 36.9 to 46.78 GeV. Noting that at the highest energy the cross section is large, we have investigated these data in detail. In Fig. 10 we give the differential cross section of inclusive muon events as a function of thrust. The energy interval for these data points is 36.9 GeV $\leq \sqrt{s} \leq 46.3$ GeV. Monte Carlo simulations with 5 flavors and 6 flavors are shown in solid and dashed histograms, respectively. In the dashed histogram, we take the top-quark mass to be 20.5 GeV. The 5-flavor prediction and the data agree. The effect of the top quark in the 6-flavor prediction is a sizable contribution at low-thrust values which is absent from the data. The total integrated luminosity is 30 pb^{-1}.

Figure 11 shows the highest-energy data, $46.3 \leq \sqrt{s} \leq 46.78$ GeV, with a luminosity of 2.8 pb^{-1}. The histo-

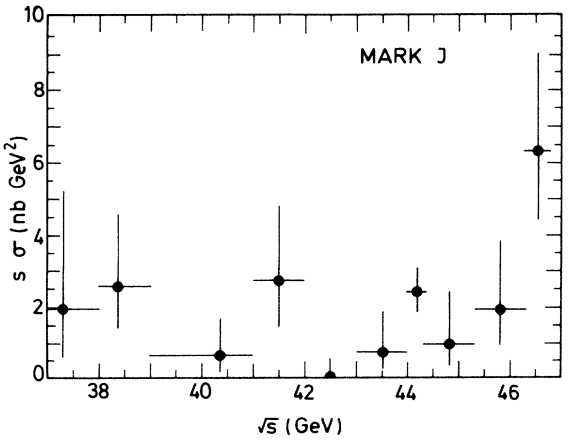

FIG. 9. The cross section of inclusive muon events with thrust < 0.8 as a function of c.m. energy $\sqrt{s}$.

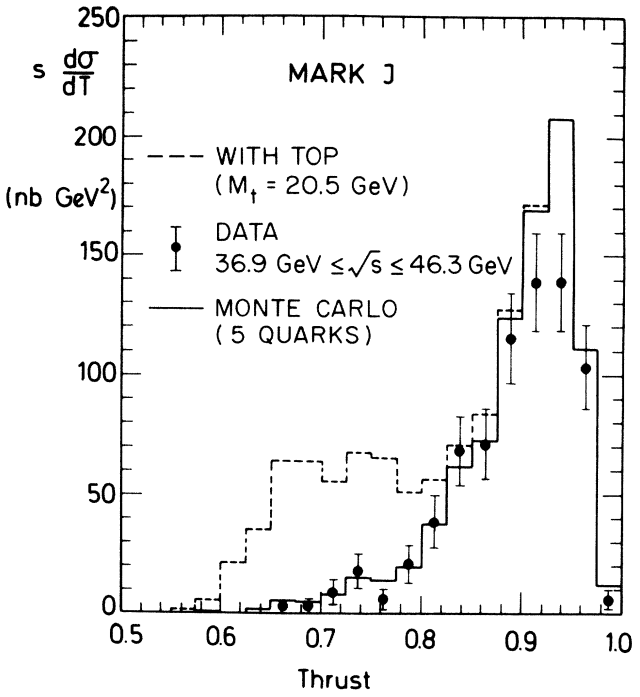

FIG. 10. Thrust distribution of events from $e^+e^- \rightarrow \mu$ + hadrons at $36.9 \leq \sqrt{s} \leq 46.3$ GeV. The predictions for 5 quarks and 6 quarks including a top quark are also shown.

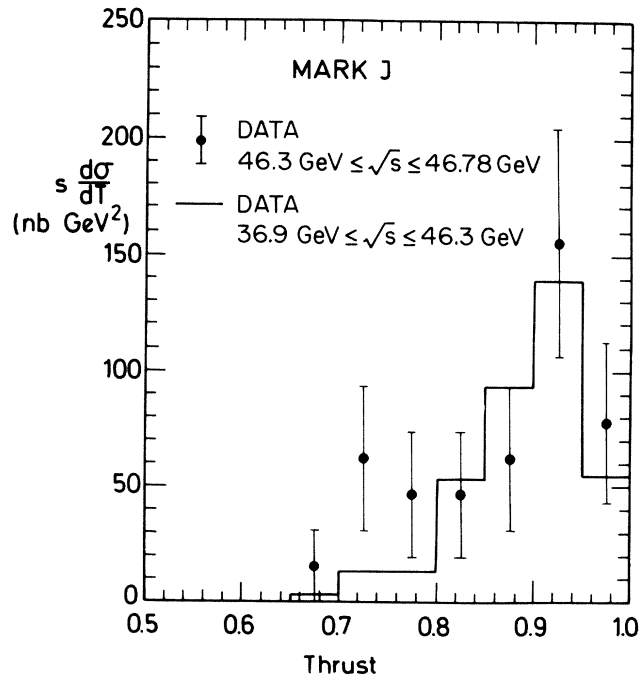

FIG. 11. Thrust distribution of events from $e^+e^- \rightarrow \mu$ + hadrons at $46.3 \leq \sqrt{s} \leq 46.78$ GeV. The measurements are compared to the lower-energy data shown in Fig. 10.

gram in this figure is the data from the lower-energy interval. In this higher-energy interval, the cross section for thrust values below 0.8 is larger than in the lower-energy region. The actual number of low-thrust events is 8, whereas 1.9 are expected from the rate at lower energy. In addition we find that the muons in these 8 events are isolated from the hadronic and electromagnetic energy flow. Figure 12 shows the energy flow of each event and indicates the energy and position of the muon with respect to the energy flow. It is remarkable that the muon never overlaps with the most energetic jet or energy cluster.

We have also investigated whether isolated muons are observed in our data at lower energies. In order to compare both data sets we calculate the angle δ of a muon track with respect to the thrust axis. Figures 13(a) and 13(b) show the correlation between the angle δ and the

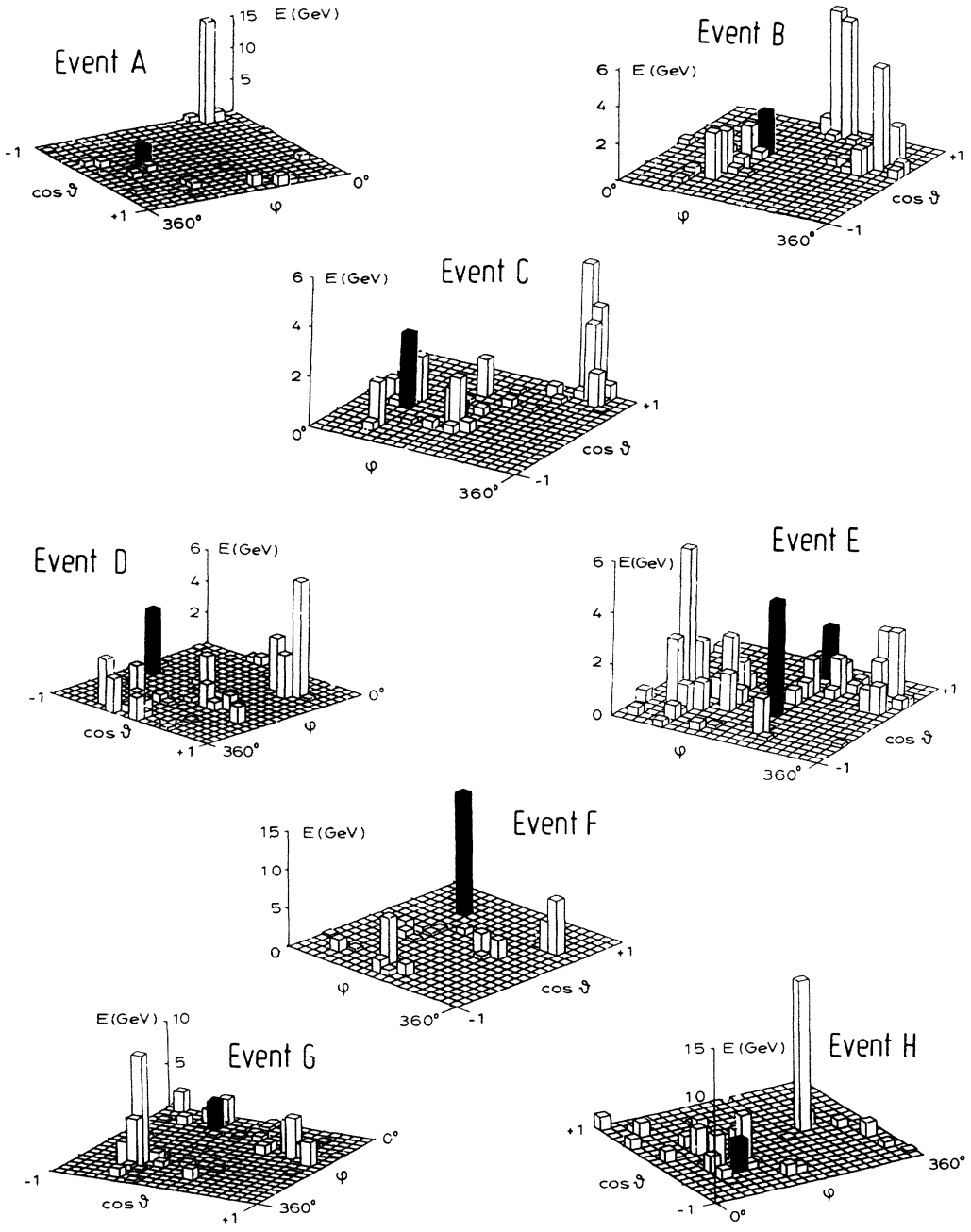

FIG. 12. Spatial distribution of the energy flow of the eight low-thrust inclusive muon events. The polar angle θ and the azimuthal angle ϕ are defined with respect to the beam line. The position and energy of a muon is marked by a black tower. The energy scale is different for each event. Event E has two muons.

thrust value for the events in the low- and high-energy samples. We see that all 8 events observed at high energies with thrust less than 0.8 could have been found as well by a cut, $\cos\delta < 0.7$. We observed 7 events at lower energies with $\cos\delta < 0.7$. Using this number and accounting for differences in the luminosity and the cross section, we would expect 0.5 events at the higher energy, $\sqrt{s} \geq 46.3$ GeV. If this cut were not *a posteriori*, the observed excess would be statistically significant. Note that the exact value of the cut in $\cos\delta$ is not critical and that the numbers of events observed at high energies in the remaining three quadrants of Fig. 13(b) agree well with those predicted from lower-energy data.

We can exhibit the muon isolation in another fashion. Below $\sqrt{s} = 46.3$ GeV the muon is typically in a region of large hadronic energy: usually in a jet for the control sample. In contrast, in the eight events above 46.3 GeV, the muon is isolated from the large hadronic energy clusters in the event. In Fig. 14 we give the differential cross section as a function of a thrustlike quantity T_μ which we define as the thrust of an event where the muon axis is used as the thrust axis. The limits on T_μ are from 0 to 1. For muons in the hadronic jets, one expects large-T_μ values. In Fig. 14, we have plotted the inclusive muon events from the highest energies as a histogram; those from the control sample as a dashed-line histogram. There is an excess in the region $T_\mu < 0.7$. The 8 events are indicated by cross hatching.

We have examined data in this and in neighboring energy regions to see if the events are due to imperfections in the detector. These events have a clean vertex inside the beam-beam interaction region. The signals from the muon trigger counter coincide with the bunch crossing signal from PETRA. Both measurements show that the events are not background from one of the beams, nor

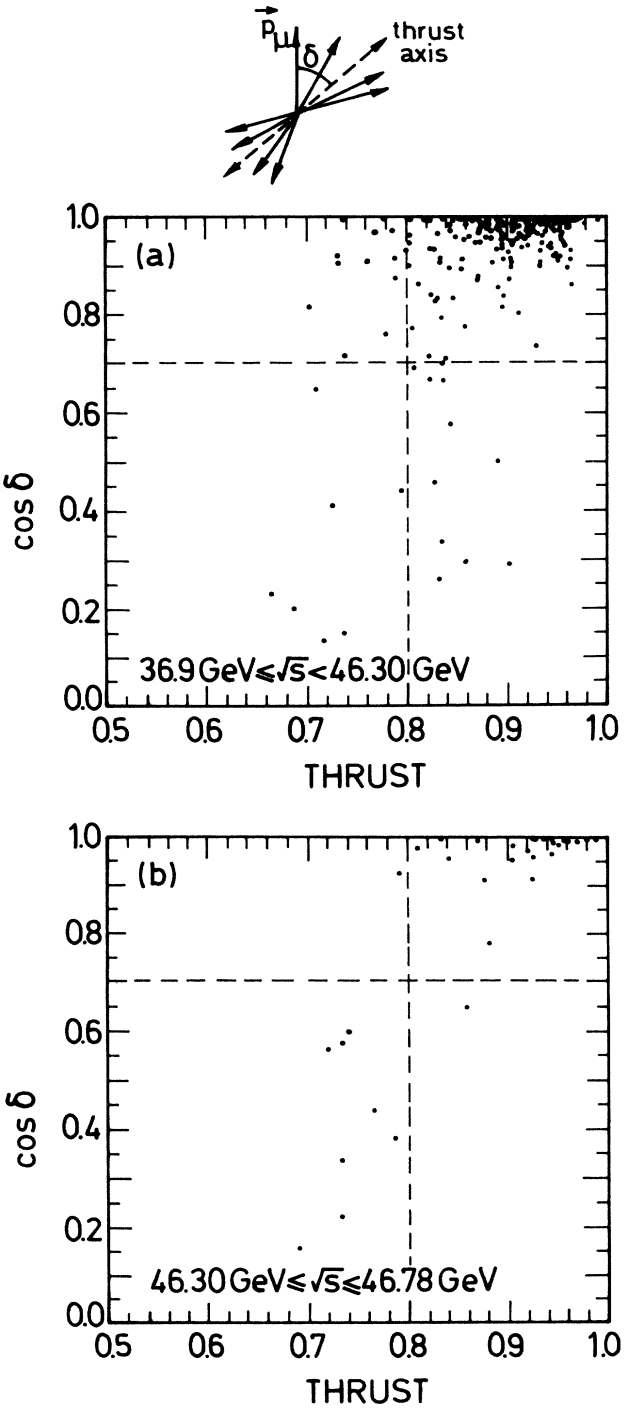

FIG. 13. (a) Scatter plot in thrust and $\cos\delta$ (δ is the angle between the muon and the thrust axis) for data in the energy band $36.9 \leq \sqrt{s} \leq 46.36$ GeV. Dashed lines indicate cuts in thrust at 0.8 and $\cos\delta$ at 0.7; (b) same as (a) but for the energy band $46.3 \leq \sqrt{s} \leq 46.78$ GeV.

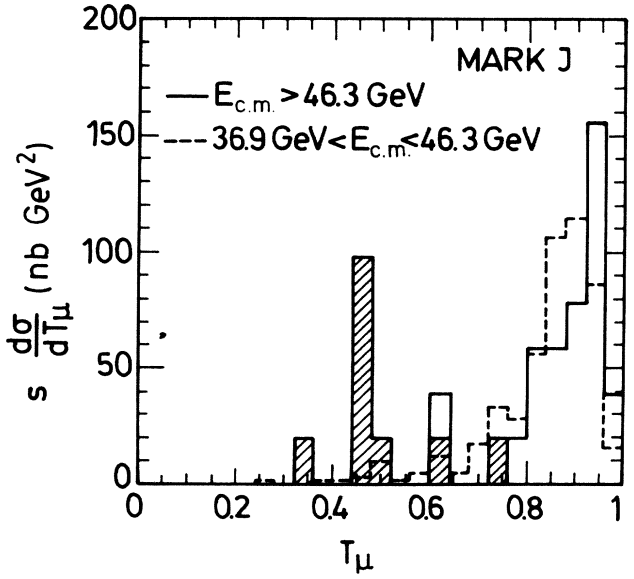

FIG. 14. The differential cross section, $s\,d\sigma/dT_\mu$, is given as a function of thrust T_μ, where the thrust direction is defined by the measured muon direction. The high-energy data is shown in the solid histogram. The 8 events are indicated by cross hatching. The low-energy data, normalized, is shown by the dashed histogram.

from cosmic rays. A most important consideration is the quality of the muon identification, as this is a potential source of background. The background of events simulated by punchthrough muons was calculated by a detailed Monte Carlo program[21] and found to be small. It does not rise significantly from 43 to 46.78 GeV. Another fact is that punch through muons are typically found in the midst of hadron jets, whereas in these 8 events the muons are isolated from the main clusters of energy. Nonprompt muons do not provide a significant background at lower energies (36.9–46.3 GeV) since the inclusive muon rates and thrust distributions agree with expectations from our Monte Carlo program. This should not increase appreciably for the higher-energy data.

As a further check of the quality of the event identification, we note that the operation of PETRA at such high energies was accompanied by an increased rate of beam-related noise in our detector. We investigated the effect of this noise on our data, using records of the detector contents at random beam crossing times, which are uncorrelated with our usual triggers. These "beam-gate triggers" indicated that the beam-related noise resulted only in very-low-energy depositions in the innermost counter layer, with recorded pulse heights typically smaller than the minimum required for counter data readout (50 MeV). We have also simulated the effect of such low-energy hits in our data, both for negligible energy deposition and in the loss of the time resolution of the counter hits. There was no evidence that the increase in noise from any source had affected this or any other data.

We have no satisfactory explanation for these events. For example, top production is very improbable; at full cross section we would expect 4–5 times more events than we observe. The question is whether these events are statistical fluctuations. We note that the other three PETRA experiments do not find a signal above their expected rate.[22] Since PETRA has now been modified and can no longer reach energies above 46.3 GeV, we must await future e^+e^- machines or the $\bar{p}p$ colliders to clarify the meaning of these events.

Note added. The JADE collaboration at PETRA reported at the Moriond Conference, 1986 (unpublished) an observation similar to our observation of these 8 low-thrust inclusive muon events. Using identical selection methods, they observed 5 such events in the same high-energy region, where they expected 0.5 events. Their result is now in perfect agreement with ours.

VI. SUMMARY

We summarize our results.

(1) The hadronic cross section excludes full top production to $\sqrt{s}=46.5$ GeV.

(2) In searching for the resonant t-quarkonium ground state we find $B_h\Gamma_{ee}\leq 3.00$ keV at 95% C.L.

(3) The investigation of event topology using R and thrust excludes full top production to $\sqrt{s}=46.6$ GeV.

From the total cross section, we are able to set limits on the Z^0 mass by using the world average for $\sin^2\theta_W=0.217\pm0.014$. We find at 95% C.L. $76\leq M_{Z^0}\leq 94$ GeV.

Form-factor parametrization gives cutoff parameters for quarks of $\Lambda_+>150$ GeV and $\Lambda_->350$ GeV at 95% C.L.

Among low-thrust hadron events containing muons we have eight events above 46.3 GeV. This very large excess remains unexplained.

ACKNOWLEDGMENTS

We thank the DESY management and the PETRA machine group for their support and effort. We also would like to thank Dr. G. Altarelli, Dr. L. Brown, Dr. G. Schierholz, Dr. F. Gutbrod, Dr. G. Kramer, Dr. T. Sjöstrand, Dr. P. Soeding, Dr. A. Ali, Dr. T. Gottschalk, Dr. R. Field, Dr. T. Walsh, and Dr. R. K. Ellis for many useful discussions. The work at the Technische Hochschule was supported by the Deutsches Bundesministerium fuer Forschung und Technologie. Some of the authors (S.A., M.H., K.N., M.F.W.) were supported by the Pakistan Atomic Energy Commission. This work was supported in part by the U. S. Department of Energy under Contract No. de-ac02-76er03069.

*Present address: Deutsches Elektronen Synchrotron, Notkestrasse, D-200 Hamburg 52, Federal Republic of Germany.

[1]For complete summaries of results at lower energies, up to the end of 1983, including references, see (a) Mark J Collaboration, Phys. Rep. **109**, 131 (1984); (b) S. L. Wu, *ibid.* **107**, 59 (1984).

[2]S. L. Glashow, Nucl. Phys. **22**, 579 (1961); S. Weinberg, Phys. Rev. Lett. **19**, 1264 (1967); Phys. Rev. D **5**, 1412 (1972); A. Salam, in *Elementary Particle Theory: Relativistic Groups and Analyticity (Nobel Symposium No. 8)*, edited by N. Svartholm (Almqvist and Wiksell, Stockholm, 1968), p. 361; S. L. Glashow, J. Iliopoulos, and L. Maiani, Phys. Rev. D **2**, 1285 (1970).

[3]Y. Nambu, in *Preludes in Theoretical Physics*, edited by A. Deshalit (North-Holland, Amsterdam, 1966), p. 133; H. Fritsch and M. Gell-Mann, in *Proceedings of the XVI International Conference on High Energy Physics, Chicago, 1972*, edited by J. D. Jackson and A. Roberts (Fermi National Accelerator Laboratory, Batavia, Illinois, 1973), Vol. 2, p. 135; S. Weinberg, Phys. Rev. Lett. **31**, 494 (1973); D. J. Gross and F. A. Wilczek, *ibid.* **30**, 1343 (1973); Phys. Rev. D **8**, 3633 (1973); **9**, 980 (1974); G. 't Hooft, Nucl. Phys. **B33**, 73 (1973); and for a recent review, F. Wilczek, Ann. Rev. Nucl. Part. Sci. **32**, 177 (1982).

[4]A. De Rujula *et al.*, Nucl. Phys. **B138**, 387 (1978).

[5]G. Arnison *et al.* [Phys. Lett. **147B**, 493 (1984)] report events which they interpret as possibly from decays of particles containing a top quark.

[6]H. G. Wu, M.S. thesis, Chinese University of Science and Technology, Hefei, Anhui, People's Republic of China, 1985; H. S. Chen, Ph.D. thesis, Massachusetts Institute of Technology, Cambridge, Massachusetts, 1984.

[7]B. Adeva *et al.*, Phys. Rev. Lett. **50**, 799 (1983).

[8]F. A. Berends *et al.*, Nucl. Phys. **B202**, 63 (1983).

[9]For a summary of quarkonium physics see E. Eichten, in *The Sixth Quark*, proceedings of the 12th SLAC Summer Institute

on Particle Physics, Stanford, 1984, edited by Patricia M. McDonough (SLAC, Stanford, 1985).

[10]S. Jüsken *et al.,* Report No. CERN-Th. 4106/84, 1985 (unpublished).

[11]J. Ellis and M. K. Gaillard, Report No. CERN 76-18, 1976 (unpublished); M. Dine and J. Saperstein, Phys. Rev. Lett. **43**, 668 (1979); K. G. Chetyrkin *et al.,* Phys. Lett. **85B**, 277 (1979); W. Celmaster and R. J. Gonsalves, Phys. Rev. Lett. **44**, 560 (1979); J. Jersak *et al.,* Phys. Lett. **98B**, 363 (1981).

[12]Publications on R by the PETRA groups are CELLO Collaboration, H.-J. Behrend *et al.,* Report No. DESY 81-029, 1981 (unpublished); Phys. Lett. **144B**, 297 (1984); JADE Collaboration, W. Bartel *et al.,* Phys. Lett. **88B**, 171 (1979); **89B**, 136 (1979); **91B**, 152 (1980); **100B**, 364 (1981); **129B**, 145 (1983); **160B**, 337 (1985); Mark J Collaboration, D. P. Barber *et al.,* Phys. Rev. Lett. **42**, 1113 (1979); **43**, 901 (1979); **44**, 1722 (1980); **50**, 799 (1983); Phys. Lett. **85B**, 463 (1979); see Ref. 1(a); PLUTO Collaboration, Ch. Berger *et al.,* Phys. Lett. **81B**, 410 (1979); **86B**, 413 (1979); TASSO Collaboration, R. Brandelik *et al., ibid.* **83B**, 261 (1979); **88B**, 199 (1979); **113B**, 499 (1982); Z. Phys. C **4**, 87 (1980); M. Althoff *et al.,* Phys Lett. **138B**, 441 (1984).

[13]J. R. Rosner *et al.,* Phys. Lett. **74B**, 350 (1978); M. Dreco, *ibid.* **77B**, 84 (1978); for a review, W. Buchmüller, Report No. CERN-Th. 3938/84, 1984 (unpublished).

[14]M. Krammer *et al.,* Report No. DESY 80/25, 1980 (unpublished); J. P. Leveille, in *Proceedings of the Z^0 Physics Workshop,* Ithaca, New York, 1981, edited by M. E. Peskin and S.-H. H. Tye (Laboratory of Nuclear Studies, Cornell University, Ithaca, 1981), p. 241; S. Pakvasa *et al.,* Phys. Rev. D **20**, 2862 (1979).

[15]P. B. Mackenzie and G. P. Lepage, Phys. Rev. Lett. **47**, 1244 (1981).

[16]J. D. Jackson and P. L. Scharre, Nucl. Instrum. Methods **128**, 13 (1975).

[17]B. Adeva *et al.,* Phys. Rev. Lett. **54**, 1750 (1985).

[18]The Z^0 mass measurements by the UA1 and UA2 experiments at CERN are given in the following: UA1, G. Arnison *et al.,* Phys. Lett. **166B**, 484 (1986); UA2, J. A. Appel *et al.,* Z. Phys. C **30**, 1 (1986).

[19]F.-P. Poschmann, Ph.D. thesis, Rheinisch-Westfälische Technische Hochschule, Aachen, West Germany, 1985.

[20]A. Böhm, in *Proceedings of the Electroweak Session of the XX Rencontre de Moriond, Les Arcs, France, 1985,* edited by J. Tran Thanh Van (Editions Frontieres, 1985), p. 141.

[21]H. Fesefeldt, Physikalisches Institute, Technische Hochschule, Aachen, Report No. 85/02, 1985 (unpublished).

[22]H.-J. Behrends *et al.,* Phys. Lett. **141B**, 145 (1984). The CELLO Collaboration has reported one unusual event with two isolated, energetic (>10 GeV) muons and two hadronic jets ($\sqrt{s}=43$ and 45 GeV).